New unsymmetrical donor dimethyl(ethylenedioxy)tetraselenafulvalene (DMEDO-TSeF): Structures and properties of its cation radical salts†

Takashi Shirahata,* Megumi Kibune and Tatsuro Imakubo*

Received 19th August 2005, Accepted 13th September 2005
First published as an Advance Article on the web 26th September 2005
DOI: 10.1039/b511820d

A novel unsymmetrical tetraselenafulvalene (TSeF)-type donor dimethyl(ethylenedioxy)tetraselenafulvalene (DMEDO-TSeF) has been synthesized without the use of the highly toxic reagent CSe_2 and the structures and properties of its cation radical salts with octahedral anions are described.

Donor molecules containing the ethylenedioxy group show excellent features such as high solubility towards most organic solvents and the ability to form CH···O hydrogen bonds. However, fusion of the [1,4]dioxene ring has been limited to the [1,3]dithiole and [1,3]thiaselenole units due to synthetic difficulties.[1] Among them, bis(ethylenedioxy)tetrathiafulvalene (BEDO-TTF or BO)[2] and bis(ethylenedioxy)diselenadithiafulvalene (BEDO-STF)[3] containing two ethylenedioxy groups on the edges of the molecular framework have been recognized as providing stable organic metals, and two superconductors have been discovered from BO salts.[4] Recently, we have achieved the first synthesis of bis(ethylenedioxy)tetraselenafulvalene (BEDO-TSeF) without the use of highly hazardous CSe_2. It is the most promising ethylenedioxy group-containing donor for the development of organic metals and superconductors, and we showed that its crystal structure and electrochemical properties are successfully inherited from the parent molecules of bis(ethylenedithio)tetraselenafulvalene (BETS)[5] and BO.[6] On the other hand, several unsymmetrical donors with one ethylenedioxy group have also been synthesized. However, almost all their cation radical salts have possessed an unstable metallic nature except for a few examples.[7] In order to stabilize the metallic nature, we have designed a new unsymmetrical TSeF-type donor DMEDO-TSeF, which is a hybrid molecule between tetramethyltetraselenafulvalene (TMTSF)[8] and BEDO-TSeF. In this communication, we report the synthesis of DMEDO-TSeF together with the structures and physical properties of its cation radical salts of octahedral anions (PF_6, AsF_6 and SbF_6).

The coupling reaction of selone **2** should be conducted under mild conditions, *i.e.* hexamethylphosphorous triamide (HMPT)–benzene at room temperature, since the C–Se bonds are weakened by the electron-donating ability of the dioxene ring.[6] In the course of our study to investigate the application of the above mild conditions for the formation of the central double bond, we found that it is applicable to the coupling reaction of various kinds of selone. In fact, the coupling reaction of **1** with HMPT afforded TMTSF at a moderate yield (14%). We applied these mild conditions to the synthesis of DMEDO-TSeF (Scheme 1) and the following best result was obtained; to a mixture of selone **1** (215 mg, 0.71 mmol) and selone **2** (226 mg, 0.68 mmol) in benzene (90 mL) was added HMPT (0.74 mL, 4.08 mmol), and the solution was stirred for 2 h at room temperature. After the removal of the solvent under reduced pressure, the crude products were separated by column chromatography ($SiO_2/CS_2–CH_2Cl_2$) and then purified by preparative gel permeation chromatography (GPC/CS_2). The target DMEDO-TSeF was isolated as purple-red needles (31 mg, 0.065 mmol, 10%) together with the self-coupling products TMTSF (8%) and BEDO-TSeF (11%). The molecular structure of the DMEDO-TSeF was characterized by NMR, MS, IR, elemental analysis and X-ray structure analysis.‡§ Table 1 summarizes the half-wave potentials of DMEDO-TSeF and the related symmetrical donors measured under the same conditions. DMEDO-TSeF showed two reversible redox waves, and the first half-wave potential and ΔE value of DMEDO-TSeF lies midway between those of TMTSF and BEDO-TSeF.

The black needle crystals of $(DMEDO\text{-}TSeF)_2X$ (X = PF_6, AsF_6 and SbF_6) were prepared by the galvanostatic oxidation (0.5 μA) of DMEDO-TSeF (*ca.* 5 mg) in the presence of the

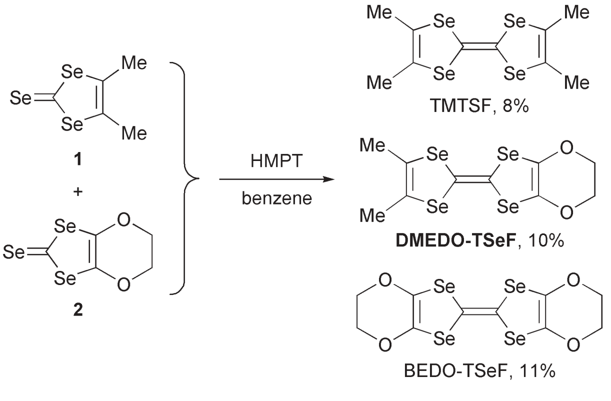

Scheme 1 Synthesis of DMEDO-TSeF.

Table 1 Half-wave potentials of DMEDO-TSeF and related analogues[a]

Donor	$E^1_{1/2}$/V	$E^2_{1/2}$/V	$\Delta E = E^2_{1/2} - E^1_{1/2}$
TMTSF	−0.01	+0.35	0.36
DMEDO-TSeF	+0.04	+0.35	0.31
BEDO-TSeF	+0.08	+0.34	0.26

[a] *vs.* $Cp_2Fe–Cp_2Fe^+$ couple, in PhCN with 0.1 M *n*-Bu_4NBF_4, glassy carbon working electrode, 100 mV s^{-1}, room temperature.

Imakubo Initiative Research Unit, RIKEN, 2-1 Hirosawa, Wako, Saitama 351-0198, Japan. E-mail: tsirahat@riken.jp; imakubo@riken.jp

† Electronic supplementary information (ESI) available: experimental details of the synthesis of DMEDO-TSeF, crystal structure analysis for neutral DMEDO-TSeF and band calculation for $(DMEDO\text{-}TSeF)_2X$ (X = PF_6, AsF_6 and SbF_6). See DOI: 10.1039/b511820d

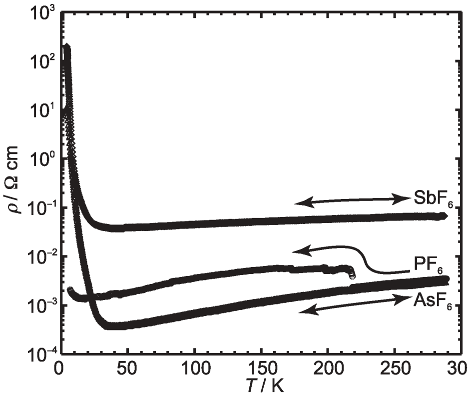

Fig. 1 Temperature dependence of the resistivity for (DMEDO-TSeF)$_2$X; X = PF$_6$, AsF$_6$ and SbF$_6$.

corresponding tetra-*n*-butylammonium salts (*ca.* 40 mg) as a supporting electrolyte in chlorobenzene (20 mL). All these salts are crystallized in a triclinic β-type structure;§ however, their conducting properties and donor arrangements are influenced by the size of the counter anion. Fig. 1 shows the temperature dependence of the resistivity for these salts. The PF$_6$ salt is metallic down to 215 K, and then a distinct phase transition occurred following the resistivity jump. Below the transition temperature, the metallic behavior remained down to *ca.* 10 K; however, the single crystals of the PF$_6$ salt were extremely fragile after the phase transition. Owing to the fragility of this type of single crystal, it is always difficult to measure resistivity at low temperature.[7d,9] Therefore, it has not been possible to measure the warming process of the temperature dependence of the resistivity in spite of many efforts, *e.g.* a very slow cooling/warming rate (0.1 K min^{-1}). On the other hand, the AsF$_6$ and SbF$_6$ salts showed metal–semiconductor transition around 40 K.

Fig. 2 shows the temperature dependence of the static magnetic susceptibility for the PF$_6$ salt. The room temperature value of χ is 2.9 × 10^{-4} emu mol^{-1}, which is appropriate for the Pauli paramagnetism of common organic metals. With the lowering of the temperature, the static magnetic susceptibility of the PF$_6$ salt decreased gradually and showed an upturn at 235 K. The temperature showing the maximum susceptibility (215 K) agrees with the transition temperature observed in the resistivity measurements. The Pauli-like behavior remained below the transition temperature and huge hysteresis was observed in the range of 215–270 K, indicating that this phase transition is a first-order metal–metal transition.

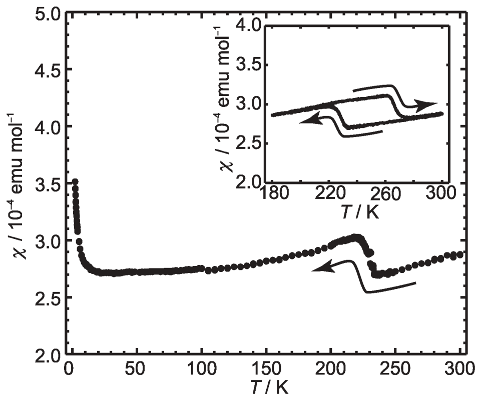

Fig. 2 Temperature dependence of the static magnetic susceptibility for (DMEDO-TSeF)$_2$PF$_6$ with an applied field of 10 kOe. The inset shows cooling and warming data around the transition temperature.

We have performed X-ray crystal structure analyses of these three salts at room temperature (293 K). The unit cell contains two donor molecules and one counter anion, giving donor to anion ratio of 2 : 1. As shown in Fig. 3, the donor molecules of these salts stack in a head-to-tail manner along the *a*-axis and are connected by short Se···Se contacts shorter than the sum of the van der Waals radii[10] along the *b*-axis. This packing diagram resembles that of the (TMTSF)$_2$X system[11] and affords quasi one-dimensional Fermi surfaces (refer to the electronic supplementary information). The donor arrangement for these three salts depends on the anion size, and there is a distinct difference in inter-column interaction. In the PF$_6$ salt, the donor molecules are aligned along the *b*-axis with a slipping distance of 4.7 Å. On the other hand, the slipping distances of the AsF$_6$ and SbF$_6$ salts are 3.2 Å in either salt. It is considered that this structural difference affects their conducting properties and that the large slips of donor molecules

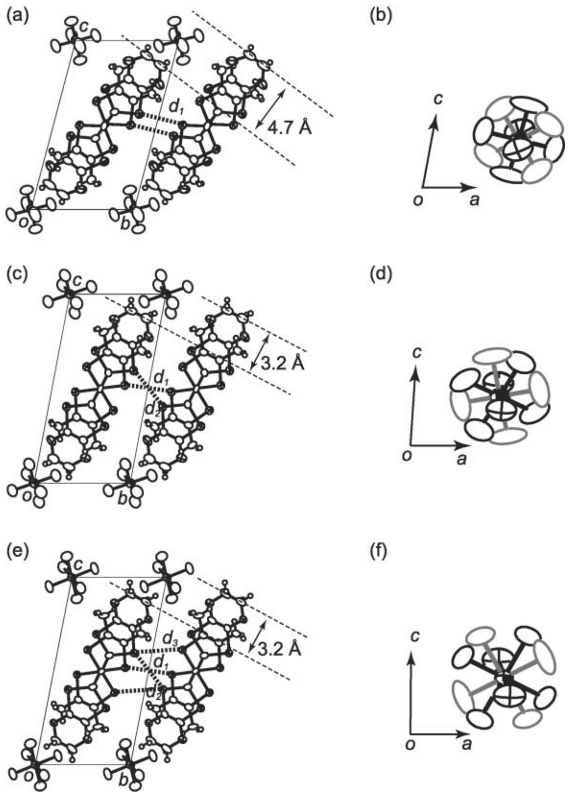

Fig. 3 Crystal structure for (DMEDO-TSeF)$_2$X at 293 K; (a), (b) X = PF$_6$, (c), (d) X = AsF$_6$ and (e), (f) X = SbF$_6$ viewed along the crystallographic *a*-axis for (a), (c) and (e), and projection on to the *ac*-plane for (b), (d) and (f). The dotted lines indicate Se···Se contacts shorter than sum of the van der Waals radii [PF$_6$: d_1 = 3.680(1) Å; AsF$_6$: d_1 = 3.680(2), d_2 = 3.645(2) Å; SbF$_6$: d_1 = 3.629(2), d_2 = 3.582(2), d_3 = 3.726(1) Å]. In (a), (c) and (e), the minor orientations of anions are omitted for clarity. In (b), (d) and (f), the ordered and disordered fluorine atoms are represented with axes and open ellipsoids, respectively, and the major and minor orientations are showed by the black and gray lines, respectively [PF$_6$: 0.55(5)/0.45(5); AsF$_6$: 0.51(5)/0.49(5); SbF$_6$: 0.67(4)/0.33(4)].

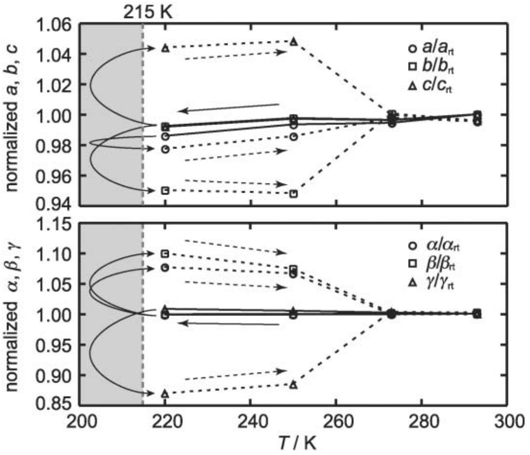

Fig. 4 Temperature dependence of the cell parameters for (DMEDO-TSeF)$_2$PF$_6$. The values of cell parameters are normalized to their respective values at 293 K. The solid and broken lines indicate the cooling and warming process, respectively.

observed in the PF$_6$ salt play an important role in first-order metal–metal transition (*vide infra*). The anions of these three salts were taken in a cavity formed by the zigzag-type donor stacks and showed disorder based on uni-axial rotation. In the SbF$_6$ salt, the motion of the octahedral anion is a jiggle rather than a rotation because large SbF$_6$ anions are installed in the cavity more precisely.

The unit cell parameters of the PF$_6$ salt have been measured at various temperatures from 293 to 220 K. As shown in Fig. 4, the values of cell parameters *a*, *b* and *c* regularly decrease with temperature down to 220 K due to thermal contraction. We tried to perform structure analysis at 200 K (below the transition temperature of 215 K) in order to investigate the low-temperature metallic phase. However, the refinement of the cell parameters was unsuccessful due to the appearance of many incommensurate reflections. In the warming process, coherence of the crystals was recovered above 215 K, and the cell parameters showed drastic change due to the generation of a new phase. The cell parameters of the PF$_6$ salt at 220 K are summarized in Table 2 compared with the room temperature values of the PF$_6$, AsF$_6$ and SbF$_6$ salts. It is interesting that the new phase observed in the warming process is isostructural with the AsF$_6$ and SbF$_6$ salts and it should be also noted that the drastic changes of the unit cell angles are characteristic in this phase transition. According to preliminary structure refinement, the slipping distance between neighboring donor molecules diminished to 3.2 Å from the room temperature value of 4.7 Å. Therefore, the structural change is not simple thermal contraction but the molecules glide by 1.5 Å along the molecular long axis. As a result of this immense structural change, it is quite reasonable that the single crystals are extremely fragile during phase transition.

Table 2 Comparison of the cell parameters between the room and low-temperature phases of PF$_6$ salt and the room-temperature phase of AsF$_6$ and SbF$_6$ salts

	PF$_6$	PF$_6$	AsF$_6$	SbF$_6$
T/K	293	220[a]	293	293
a/Å	7.302(3)	7.178(4)	7.269(3)	7.281(3)
b/Å	7.977(3)	7.623(5)	7.632(3)	7.930(3)
c/Å	13.500(6)	14.174(8)	14.345(6)	14.519(5)
α/deg	73.739(10)	79.375(12)	78.664(8)	79.806(8)
β/deg	79.794(8)	87.655(14)	86.234(8)	89.564(9)
γ/deg	79.329(10)	68.949(13)	69.542(7)	65.582(7)
V/Å^3	735.2(5)	711.2(7)	731.1(5)	749.2(4)

[a] Warming process.

In summary, we have successfully synthesized a new unsymmetrical donor DMEDO-TSeF without the use of highly toxic reagents. Novel organic metals with octahedral anions have been prepared and their crystal structure and physical properties have been investigated. Among them, the first-order phase transition observed in the PF$_6$ salt at 215 K will attract much interest not only as a phenomenon of basic science but also as a building block for a molecular device because of the huge molecular motion (1.5 Å per molecule) during phase transition and the wide temperature range of hysteresis.[12,13] Further studies on the physical properties of (DMEDO-TSeF)$_2$X are now in progress together with the exploration of related materials.

Notes and references

‡ *Selected data* of new compound **DMEDO-TSeF**: purple-red needles, mp 199 °C (decomp.); *m*/*z* (EI, 70 eV): 480 (M$^+$ for $C_{10}H_{10}O_2{}^{78}Se^{80}Se_3$); δ_H (270 MHz, CD_2Cl_2) 4.27 (4H, s, OCH_2CH_2O), 2.00 (6H, s, CH_3); IR (neat, *v*/cm^{-1}) 1624 (s), 1443 (m), 1368 (m), 1268 (m), 1240 (w), 1134 (s); Elemental analysis: Calc. for $C_{10}H_{10}O_2Se_4$: C, 25.13; H, 2.11. Found: C, 25.14; H, 2.11%.

§ *Crystal data* for **DMEDO-TSeF**: $C_{10}H_{10}O_2Se_4$, M = 478.02, purple-red needles (0.50 × 0.06 × 0.05 mm), monoclinic, $P2_1/c$ (#14), a = 13.958(4), b = 8.285(2), c = 11.867(3) Å, β = 109.478(6)°, V = 1293.8(6) Å^3, μ = 11.323 mm^{-1}, Z = 4, 9395 reflections measured, 3223 unique (R_{int} = 0.0571). Final R indices [$I > 2\sigma(I)$]: $R1$ = 0.0501, $wR2$ = 0.1262. *GOF* = 1.076. *Crystal data* for **(DMEDO-TSeF)$_2$PF$_6$**: $C_{20}H_{20}O_4Se_8PF_6$, M = 1101.01, black needles (0.20 × 0.05 × 0.02 mm), triclinic, $P\bar{1}$ (#2), a = 7.302(3), b = 7.977(3), c = 13.500(6) Å, α = 73.739(10), β = 79.794(8), γ = 79.329(10)°, V = 735.2(5) Å^3, μ = 10.062 mm^{-1}, Z = 1, 5474 reflections measured, 3607 unique (R_{int} = 0.0935). Final R indices [$I > 2\sigma(I)$]: $R1$ = 0.0504, $wR2$ = 0.1176. *GOF* = 0.847. *Crystal data* for **(DMEDO-TSeF)$_2$AsF$_6$**: $C_{20}H_{20}O_4Se_8AsF_6$, M = 1144.96, black needles (0.50 × 0.03 × 0.02 mm), triclinic, $P\bar{1}$ (#2), a = 7.269(3), b = 7.632(3), c = 14.345(6) Å, α = 78.664(8), β = 86.234(8), γ = 69.542(7)°, V = 731.1(5) Å^3, μ = 11.187 mm^{-1}, Z = 1, 4486 reflections measured, 3177 unique (R_{int} = 0.0351). Final R indices [$I > 2\sigma(I)$]: $R1$ = 0.0718, $wR2$ = 0.1872. *GOF* = 0.942. *Crystal data* for **(DMEDO-TSeF)$_2$SbF$_6$**: $C_{20}H_{20}O_4Se_8SbF_6$, M = 1191.79, black needle (0.40 × 0.03 × 0.02 mm), triclinic, $P\bar{1}$ (#2), a = 7.281(3), b = 7.930(3), c = 14.519(5) Å, α = 79.806(8), β = 89.564(9), γ = 65.582(7)°, V = 749.2(4) Å^3, μ = 10.702 mm^{-1}, Z = 1, 5603 reflections measured, 3688 unique (R_{int} = 0.0586). Final R indices [$I > 2\sigma(I)$]: $R1$ = 0.0652, $wR2$ = 0.1442. *GOF* = 0.862. CCDC reference numbers 281658–281661. For crystallographic data in CIF format see DOI: 10.1039/b511820d

1 H. Yamochi, in *TTF Chemistry—Fundamentals and Applications of Tetrathiafulvalene: Oxygen analogues of TTFs*, ed. J. Yamada and T. Sugimoto, Kodansha & Springer, Tokyo, 2004, ch. 4.
2 T. Suzuki, H. Yamochi, G. Srdanov, K. Hinkelmann and F. Wudl, *J. Am. Chem. Soc.*, 1989, **111**, 3108–3109.
3 T. Imakubo and K. Kobayashi, *J. Mater. Chem.*, 1998, **8**, 1945–1947.
4 (*a*) M. A. Beno, H. H. Wang, A. M. Kini, K. D. Carlson, U. Geiser, W. K. Kwok, J. E. Thompson, J. M. Williams, J. Ren and M.-H. Whangbo, *Inorg. Chem.*, 1990, **29**, 1599–1601; (*b*) S. Kahlich, D. Schweitzer, I. Heinen, S. E. Lan, B. Nuber, H. J. Keller, K. Winzer and H. W. Helberg, *Solid State Commun.*, 1991, **80**, 191–195.
5 R. R. Schumaker, V. Y. Lee and E. M. Engler, *J. Phys. (Paris)*, 1983, **44**, C3-1139–1145.
6 T. Imakubo, T. Shirahata and M. Kibune, *Chem. Commun.*, 2004, 1590–1591.
7 (*a*) A. M. Kini, T. Mori, U. Geiser, S. M. Budz and J. M. Williams, *J. Chem. Soc., Chem. Commun.*, 1990, 647–648; (*b*) J.-M. Fabre,

D. Serhani, K. Saoud, S. Chakroune and M. Hoch, *Synth. Met.*, 1993, **60**, 295–298; (*c*) T. Imakubo, Y. Okano, H. Sawa and R. Kato, *J. Chem. Soc., Chem. Commun.*, 1995, 2493–2494; (*d*) J.-M. Fabre, A. Javidan, L. Binet, J. Ramos and P. Delhaes, *Synth. Met.*, 1997, **86**, 1889–1890; (*e*) A. Ota, H. Yamochi and G. Saito, *J. Mater. Chem.*, 2002, **12**, 2600–2602.

8 K. Bechgaard, D. O. Cowan and A. N. Bloch, *J. Chem. Soc., Chem. Commun.*, 1974, 937–938.

9 E. Laukhina, J. Vidal-Gancedo, V. Laukhin, J. Veciana, I. Chuev, V. Tkacheva, K. Wurst and C. Rovira, *J. Am. Chem. Soc.*, 2003, **125**, 3948–3953.

10 A. Bondi, *J. Phys. Chem.*, 1964, **68**, 411–451.

11 K. Bechgaard, C. S. Jacobsen, K. Mortensen, H. J. Pedersen and N. Thorup, *Solid State Commun.*, 1980, **33**, 1119–1125.

12 T. Ishiguro, K. Yamaji and G. Saito, *Organic Superconductors*, Springer, New York, 1998.

13 For a recent application of a phase transition in organic conductors to a molecular device, see: M. Chollet, L. Guerin, N. Uchida, S. Fukaya, H. Shimoda, T. Ishikawa, K. Matsuda, T. Hasegawa, A. Ota, H. Yamochi, G. Saito, R. Tazaki, S. Adachi and S. Koshihara, *Science*, 2005, **307**, 86–89.